

Hot-stage transmission electron microscopy study of (Na, K)NbO₃ based lead-free piezoceramics

Cite as: Appl. Phys. Lett. **105**, 042904 (2014); <https://doi.org/10.1063/1.4891960>

Submitted: 18 June 2014 . Accepted: 20 July 2014 . Published Online: 30 July 2014

Shengbo Lu, Zhengkui Xu, K. W. Kwok, and Helen L. W. Chan



View Online



Export Citation



CrossMark

ARTICLES YOU MAY BE INTERESTED IN

High piezoelectric activity in (Na,K)NbO₃ based lead-free piezoelectric ceramics: Contribution of nanodomains

Applied Physics Letters **99**, 062901 (2011); <https://doi.org/10.1063/1.3624704>

Large piezoelectricity in Pb-free 0.96(K_{0.5}Na_{0.5})_{0.95}Li_{0.05}Nb_{0.93}Sb_{0.07}O₃-0.04BaZrO₃ ceramic: A perspective from microstructure

Journal of Applied Physics **117**, 084106 (2015); <https://doi.org/10.1063/1.4913454>

Piezoelectric properties of Li- and Ta-modified (K_{0.5}Na_{0.5})NbO₃ ceramics

Applied Physics Letters **87**, 182905 (2005); <https://doi.org/10.1063/1.2123387>

Lock-in Amplifiers
Find out more today



Zurich
Instruments

Hot-stage transmission electron microscopy study of (Na, K)NbO₃ based lead-free piezoceramics

Shengbo Lu,^{1,2,a)} Zhengkui Xu,¹ K. W. Kwok,² and Helen L. W. Chan²

¹Department of Physics and Materials Science, City University of Hong Kong, 83 Tat Chee Avenue, Kowloon, Hong Kong

²Department of Applied Physics and Materials Research Centre, The Hong Kong Polytechnic University, Hung Hom, Kowloon, Hong Kong

(Received 18 June 2014; accepted 20 July 2014; published online 30 July 2014)

Hierarchical nanodomains assembled into micron-sized stripe domains, which is believed to be associated with outstanding piezoelectric properties, were observed at room temperature in a typical lead free piezoceramics, (Na_{0.52}K_{0.48-x})(Nb_{0.95-x}Ta_{0.05})-xLiSbO₃, with finely tuned polymorphic phase boundaries ($x = 0.0465$) by transmission electron microscopy. The evolution of domain morphology and crystal structure under heating and cooling cycles in the ceramic was investigated by *in-situ* hot stage study. It is found that the nanodomains are irreversibly transformed into micron-sized rectangular domains during heating and cooling cycles, which lead to the thermal instability of piezoelectric properties of the materials. © 2014 AIP Publishing LLC.

[<http://dx.doi.org/10.1063/1.4891960>]

The development of piezoelectricity in lead-free ceramics is of much interest for human health and environmental protection. In recent years, lead-free piezoelectric materials with excellent properties have been intensively studied to find an alternative for toxic lead zirconate titanate (PZT) materials.¹⁻⁴ Among several families of lead-free piezoelectric materials (Na, K)NbO₃ (NKN) ceramics are considered to be promising candidates to replace PZT owing to the high electromechanical coupling coefficient (k_p) and high Curie temperature ($T_c \sim 420^\circ\text{C}$) of these materials.⁵ However, pure NKN ceramics generally show low piezoelectric properties compared to PZT system ceramic.⁶ As a result, various chemical modifiers, such as LiTaO₃,^{7,8} LiNbO₃,^{9,10} LiSbO₃,¹¹⁻¹³ CaZrO₃,^{14,15} and BaZrO₃,^{16,17} have been employed to facilitate processing and optimize the piezoelectric behavior. The enhanced piezoelectric properties in NKN-based ceramics are attributed to shifting the temperature of the polymorphic phase boundary (PPB), where either the tetragonal (T) and orthorhombic (O) or the tetragonal and rhombohedral (R) phases coexist, to room temperature.² For the PPB of coexistence of orthorhombic and tetragonal phase, a d_{33} of ~ 416 pC/N was recorded at room temperature,¹⁸ while for the PPB of coexistence of rhombohedral and tetragonal phase a d_{33} as high as ~ 490 pC/N has been reported in a NKN based system recently.¹⁹ However, a drawback of the PPB is temperature sensitivity, which is one of the bottlenecks for device application despite of the high piezoelectric properties at room temperature. Zhang *et al.* reported that for LiSbO₃ doped NKN ceramics, a drop of d_{33} from 355 pC/N to 250 pC/N when heating from room temperature to 50°C .¹³ Yao *et al.* also demonstrated that d_{33} decreases monotonically with elevated temperature, and 40% reduction of d_{33} occurs in (K,Na,Li)(Nb,Ta,Sb)O₃ ceramics when heating to 120°C .²⁰ Akdoğan *et al.* found that for LiTaO₃ and LiSbO₃

co-doped NKN ceramics the spontaneous polarization P_s , permittivity and piezoelectric coefficient d_{33} all peaked in a narrow temperature $25\text{--}31^\circ\text{C}$.²¹ Hollenstein *et al.* demonstrated that the piezoelectric coefficient d_{31} and k_p decreased up to 30% of their initial value after the first heating and cooling cycle up to 140°C for Li-modified NKN. However, after the second cycle, the property stabilized.²² Ideally, the room temperature properties of a piezoelectric material are expected to be recovered after repeated thermal cycle in devices because inevitable temperature fluctuation will happen during either device fabrication or device application. For example, medical probes containing piezoelectric transducer sometimes need to be sterilized at temperatures above 100°C . Despite that some progresses have been made to improve the thermal stability of NKN based lead free piezoceramics,^{18,23-25} the physical mechanism behind remains unknown. As a result, clarifying microstructural origin of the thermal instability of properties in NKN based piezoceramics is of a considerable practical importance.

It is well known that the piezoelectric properties of ferroelectric materials are strongly related to their ferroelectric domain structures and crystal symmetry. Therefore, the temperature dependent evolution of ferroelectric domain and phase symmetry is crucial to the understanding of microstructural origin of the thermal instability of NKN based ceramics. However, the room-temperature domain structure in NKN based ceramic has only recently been investigated by transmission electron microscopy (TEM).^{26,27} Coexistence of orthorhombic and tetragonal nanodomains was confirmed by convergent beam electron diffraction (CBED) method in NKN based piezoceramic with a PPB composition at room temperature.²⁶ Although the nanodomains, which are believed to be associated with the strong piezoelectricity, are also found in NKN based piezoceramics at room temperature, one question remains: Can these nanodomains survive in the heating and cooling cycle? In this work, domain structures of

^{a)}Electronic mail: shengbo.lu@yahoo.com

typical $(\text{Na}_{0.52}\text{K}_{0.48-x})(\text{Nb}_{0.95-x}\text{Ta}_{0.05})\text{-xLiSbO}_3$ (NKNT-xLS) lead free piezoceramics with a PPB composition ($x = 0.0465$) and a Curie temperature around 320°C (Ref. 28) are investigated by TEM. *In situ* hot stage study during two heating and cooling cycles of NKNT-0.0465LS from 25°C to 350°C reveals that the micron-sized stripe domains consisting of hierarchical nanodomains structures transform irreversibly into rectangular domains with broadened domain walls during the first heating and cooling cycle; while during second heating and cooling cycle after 24 h, only slight change of domain structures can be observed. These results are believed to be one of the reasons that a drastic degradation of piezoelectric properties was found in the first heating and cooling cycle, and followed by stabilized properties during the second cycle as observed by Hollenstein *et al.*²²

NKNT-xLS were fabricated by conventional solid state process as described in Ref. 28. The specimens for TEM observation were prepared from bulk materials by mechanical thinning to $\sim 10\ \mu\text{m}$ and then ion milling to perforation using a Gatan Dual Ion mill unit (Model 600). Specimens were coated with carbon before TEM examination. The domain morphology was examined on TEM (Philips CM-20, Hillsboro, OR) operated at 200 kV. The *in situ* heating/cooling observation was performed from room temperature to 350°C on a double-tilt heating specimen holder (Gatan Model 652) with the temperature controlled precisely by a SmartSet Hot Stage controller (Gatan Model 901). The accuracy of the temperature measurement is about 0.1°C . A heating and cooling rate less than $3^\circ\text{C}/\text{min}$ was used. Bright filed (BF) images, CBED, and selected area electron diffraction (SAED) patterns were recorded 10 min after the temperature was stabilized. The CBED and SAED patterns are indexed on the basis of the pseudo-cubic unit cell. All specimens were annealed at a temperature of 80°C for 24 h to release the stress induced during sample preparation.

Figure 1 shows typical stripe domains consisting of lamellar hierarchical nanodomain structures in NKNT-0.0465LS with a PPB composition, which have been reported both in Pb-based and Pb-free piezoceramics and are believed to be associated with the strong piezoelectricity

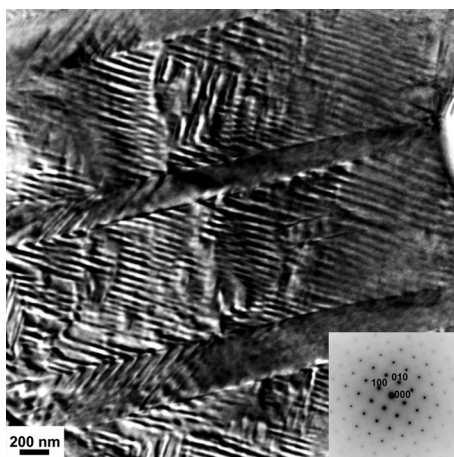


FIG. 1. BF image of typical domain configuration with micron- and nano-scale domains in NKNT-0.0465LS ceramic, viewed along $\langle 001 \rangle$ zone axis. Inset shows the SAED of the examined grain.

in those systems at room temperature. The submicron strip domains are of 200 to 900 nm in width arranged by nanodomains with a width of 50 nm. The domain orientations are examined by SAED as shown in the inset of Fig. 1. The micron-scale domain walls are along $\langle 110 \rangle$ direction, while the nanodomain walls are approximately along either $\langle 100 \rangle$ or $\langle 010 \rangle$ directions. The domain structures are quite similar to those previously reported in another NKN based piezoceramic system,²⁶ indicating a coexistence of O and T phase at room temperature in the NKNT-0.0465LS ceramic.

To understand the thermal stability of the domain structures in NKNT-0.0465LS temperature-driven domain evolution was investigated by *in situ* heating and cooling, as shown in Figs. 2(a)–2(g). In the virgin state at room temperature, both micron-sized parallel stripe domains and rectangular domains are found (Fig. 2(a)), with their domain walls tracing along $\langle 110 \rangle$ and $\langle 100 \rangle$ directions, respectively, as indicated by the SAED pattern shown in the inset of Fig. 2(a). When heating to 150°C , the contrast of the strip domains slightly changed, as indicated by the white arrows in Fig. 2(b). Meanwhile, some of the domain walls of the rectangular domains begin to disappear. It has been reported that there exists an $\text{O} \rightarrow \text{T}$ phase transition at around 35°C in NKNT-0.0465LS ceramic.²⁷ Detailed domain evolutions in the area with white frames in Fig. 2 will be further

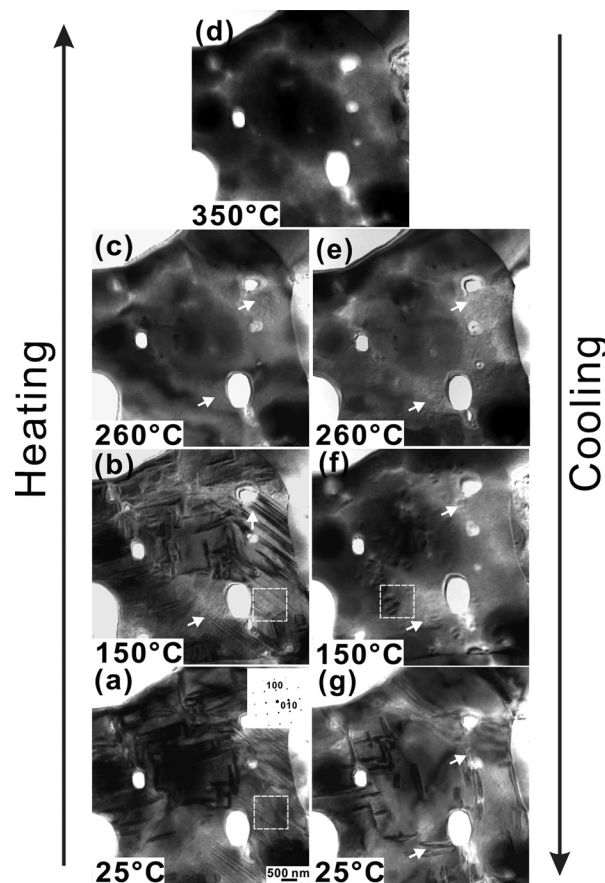


FIG. 2. *In situ* TEM observations of grain along the $\langle 001 \rangle$ zone axis in a NKNT-0.0465LS specimen during first heating and cooling cycle. BF micrographs at (a) virgin state, 25°C , (b) 150°C on heating, (c) 260°C on heating, (d) 350°C on heating, (e) 260°C on cooling, (f) 150°C on cooling, (g) 25°C on cooling. Inset in Fig. 2(a) shows the SAED of the examined grain.

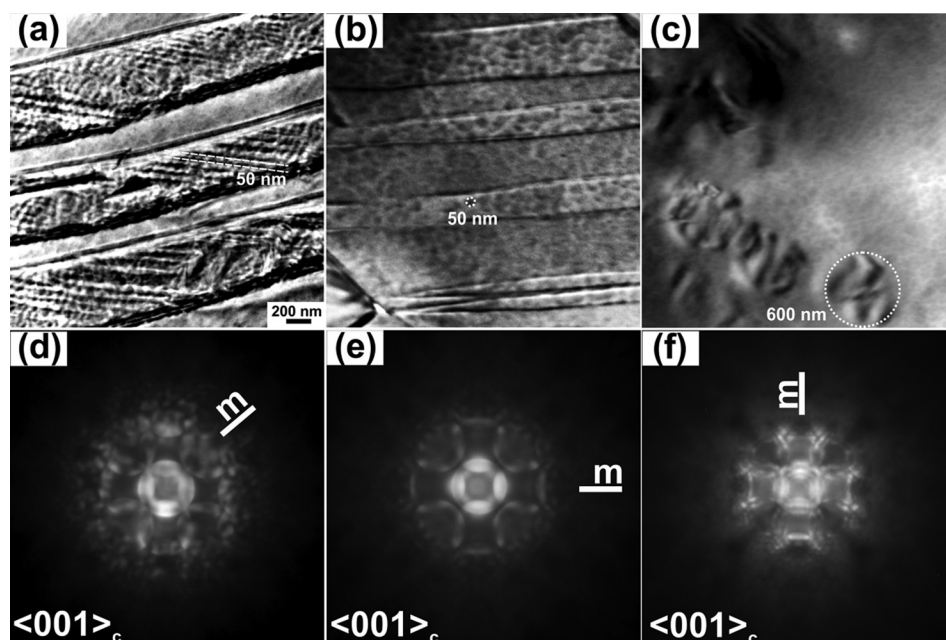


FIG. 3. High magnification view of domain structures at (a) virgin state, i.e., 25 °C, (b) 150 °C on heating, (c) 150 °C on cooling, respectively, as marked by dashed squares in Fig. 2. (d), (e), and (f) are corresponding CBED patterns taken from domains marked in (a), (b), and (c), along $\langle 001 \rangle$ zone axis. For BF images, specimen is tilted a few degrees off the $\langle 001 \rangle$ zone axis in order to view the nanodomains clearly.

illustrated in Fig. 3. With further increase of temperature to 260 °C, both the stripe and rectangular domains disappeared and transformed into nano-sized island domains, as indicated by the white arrows in Fig. 2(c). The domain contrast completely disappeared at 350 °C, as shown in Fig. 2(d), suggesting the completion of the ferroelectric to paraelectric phase transition. No changes were detected on cooling from 350 °C until 260 °C when the nano-sized island domains reappeared in the grain, as evident in Fig. 2(e). These nano-sized island domains gradually transformed into micron-sized irregular domains at 150 °C (Fig. 2(f)). It is worthwhile to note that the projections of the traces of the micron-sized irregular domains walls do not appear to orient in any principle crystallographic directions. When cooled back to 25 °C, the island domains disappeared completely leaving only the rectangular domain contrast with broadened domain walls. Clearly, the parallel stripe domains do not recover after a heating and cooling cycle. Similar rectangular domain structure was also observed in a recent *in situ* TEM study of $0.948(\text{K}_{0.5}\text{Na}_{0.5})\text{NbO}_3-0.052\text{LiSbO}_3$ under an electric field of 14 kV/cm.²⁸ It is interesting to note that significant differences of domain structures are observed before and after the first order phase transition within the temperature range in this study, as shown in Figs. 2(a) and 2(g). This can be attributed to the thermal hysteresis during the first order phase transition of the NKN based ceramic, which is evident by the coexistence of O and T phases in Fig. 2(a) while a largely T phase observed in Fig. 2(g) when cooling back from 350 °C to room temperature. As a result, the room-temperature domain structures after phase transition are markedly changed comparing to their virgin state.

Figure 3 shows the high-magnification BF micrographs of the areas indicated by dashed square in Fig. 2 to further elucidate the domain evolution during heating and cooling. At virgin state, the lamellar hierarchical nanodomains within submicron strip domains can be clearly seen with a width of around 50 nm, as shown in Fig. 3(a). When heated to 150 °C,

the hierarchical nanodomains had notably different features (Fig. 3(b)): island nanodomains of 50 nm in size became apparent within the strip domains. Although at the same temperature, a clear difference of domain morphology can be seen when the sample was cooled back to 150 °C and irregular domains with a size of 600 nm emerged and occupied the whole grain instead of stripe domains as evident in Fig. 3(c). Moreover, the symmetry of the nanodomains was examined by CBED, as shown in Figs. 3(d)–3(f). For O phases with a 2 mm symmetry, the mirror plane in $\langle 001 \rangle$ CBED patterns should be parallel to the $\langle 110 \rangle$ direction, while it should be parallel to the $\langle 100 \rangle$ direction for T phases with a 4 mm symmetry. Therefore, it turns out that the lamellar nanodomains are O phase at room temperature while the island nanodomains and the irregular domain are T phase at 150 °C. Although the composition of NKNT-0.0465LS ceramic was designed to have the coexistence of O and T phases at room temperature, the $\text{O} \rightarrow \text{T}$ phase transition was found to be diffusive, which means that the coexistence of O and T phases could be sustained in a wide temperature range.²⁷ The $\text{O} \rightarrow \text{T}$ transition boundary where the phase transition completes could be around 150 °C in this study, as indicated by the CBED analysis, which is in agreement with the previously reported one, near 130 °C.²⁹ Based on the observations during heating and cooling, as shown in Figs. 2 and 3, the domain evolution in NKNT-0.0465LS ceramic can be divided into six phases. First, upon heating, the O phase lamellar nanodomains were transformed into T phase island domains at 150 °C. Second, upon further heating, micron-sized rectangular domains and strip domains were changed into island nanodomains completely at 260 °C. Third, the domain contrast disappeared completely at 350 °C. Fourth, upon cooling, island nanodomains were emerged first at 260 °C. Fifth, upon further cooled to 150 °C, coalescence of the island nanodomains into micron-sized irregular domains appeared. Finally, the irregular domains were transformed into rectangular domains with broadened domain walls when cooled back to

room temperature. It is noteworthy that there exists a complete disappearance of lamellar nanodomains during the heating and cooling cycle, which is believed to be the reason that the marked drop of d_{33} after a heating and cooling cycle. Similar to BaTiO_3 ,³⁰ the T to O phase transition in NKN piezoceramics is proved to be a discontinuous, first-order phase transition.³¹ The polarization vector does not follow continuously the $\langle 001 \rangle$ to $\langle 101 \rangle$ but jumps abruptly from the $\langle 001 \rangle$ to the $\langle 101 \rangle$ axis at the phase transition temperature. This sudden change of polarization direction will induce a change of strain during the $T \rightarrow O/O \rightarrow T$ phase transition. As a result, domain walls will reshape to accommodate the change of strain. Accordingly, domain walls were found to be changed dynamically during the O/T phase transition.

To investigate whether the domain structure is stabilized or not after the first heating and cooling cycle, the sample was kept in TEM chamber for 24 h. Domain structure evolution under a second heating and cooling cycle was then examined in another grain along $\langle 001 \rangle$ zone axis, as illustrated in Figs. 4(a)–4(d). Fig. 4(a) shows similar rectangular domains observed in Fig. 2(g). With subsequent heating and cooling to 150 °C (Figs. 4(b) and 4(c)), only irregular domains can be seen, which are similar to domains shown in Fig. 2(f). When cooling back to room temperature, only a slight change in domain morphology can be seen as evident in Fig. 4(d) when comparing with the one before second heating and cooling cycle as shown in Fig. 4(a). The domain walls of the rectangular domains get even broader and still, stripe domains consisting of hierarchical nanodomains never recover. Other than the two $\langle 001 \rangle$ oriented grains shown in Figs. 2 and 4, many grains with various orientations have been also investigated, similar behavior is observed. Miniaturized domains due to low polarization anisotropy at the PPB and MPB boundary in ferroelectrics are believed to be associated with the strong piezoelectricity at room temperature as a reduced domain size may enable easier domain redistribution under external electric field. Unfortunately, this important feature is lost after the heat and cooling cycles

in NKN based ceramic with a PPB composition, which could lead to a deteriorated piezoelectric properties.

Our findings indicate a domain memory effect in the second heating and cooling cycle, which is significantly different from the first cycle. It can be explained by the defect symmetry conforming principle during the phase transition cycles.³² For a “fresh” ceramic, point defects distribute randomly and tend to form a cubic symmetry in the system. Such defect configuration does not provide any preference of domain alignment. Thus, no domain memory effect was achieved during the first heating and cooling cycle as shown in Fig. 2. However, a defect conforming symmetry consistent with the high temperature phase is developed when cooling through PPB and is then preserved into the low temperature one, as indicated by the white arrows in Figs. 2(e) to 2(g). A defect dipolar moment aligning along the spontaneous polarization direction of each domain will be generated.³³ Therefore, domain morphology will recover during the second heating and cooling cycle with the “recover force” provided by the defect polarization, as shown in Figs. 4(a)–4(d).

In summary, hierarchical nanodomains assembled into micron-sized stripe domains, which is believed to be associated with outstanding piezoelectric properties, were observed at room temperature in NKNT-0.0465LS piezoceramics with a PPB composition by TEM. However, *in-situ* hot stage study shows that this domain structure cannot survive in heating and cooling cycles, which leads to the drastic deterioration of the piezoelectric properties in the materials.

This work was supported by a grant from the Research Grants Council of the Hong Kong Special Administrative Region, China (Project No. 9041211) and an internal grant from The Hong Kong Polytechnic University (Project No. 1-ZVCG).

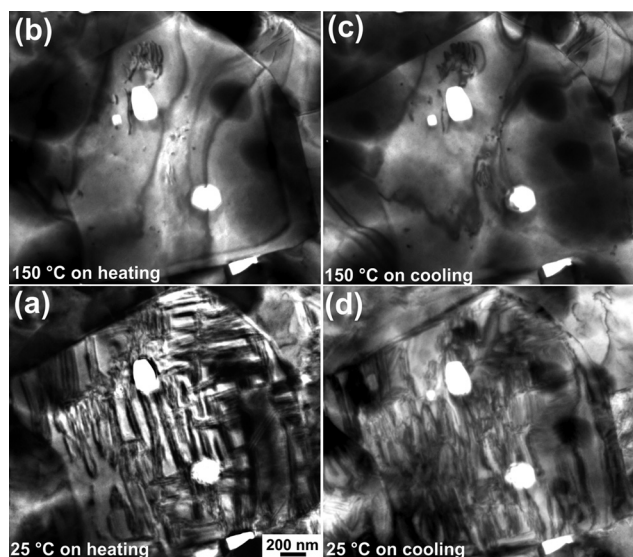


FIG. 4. BF micrographs of domain evolution in another grain along $\langle 001 \rangle$ zone axis during second heating and cooling cycle: (a) 25 °C on heating, (b) 150 °C on heating, (c) 150 °C on cooling, (d) 25 °C on cooling.

¹P. K. Panda, *J. Mater. Sci.* **44**, 5049 (2009).

²T. R. Shrout and S. J. Zhang, *J. Electroceram.* **19**, 111 (2007).

³S. O. Leontsev and R. E. Eitel, *Sci. Technol. Adv. Mater.* **11**, 044302 (2010).

⁴D. Maeder, D. Damjanovic, and N. Setter, *J. Electroceram.* **13**, 385 (2004).

⁵J. F. Li, K. Wang, F. Y. Zhu, L. Q. Cheng, and F. Z. Yao, *J. Am. Ceram. Soc.* **96**, 3677 (2013).

⁶L. Egerton and D. M. Dillon, *J. Am. Ceram. Soc.* **42**, 438 (1959).

⁷E. Hollenstein, M. Davis, D. Damjanovic, and N. Setter, *Appl. Phys. Lett.* **87**, 182905 (2005).

⁸D. Lin, K. W. Kwok, and H. L. W. Chan, *J. Appl. Phys.* **102**, 034102 (2007).

⁹K. Wang and J. F. Li, *Adv. Funct. Mater.* **20**, 1924 (2010).

¹⁰K. Wang, J. F. Li, and N. Liu, *Appl. Phys. Lett.* **93**, 092904 (2008).

¹¹G. Z. Zang, J. F. Wang, H. C. Chen, W. B. Su, C. M. Wang, P. Qi, B. Q. Ming, J. Du, L. M. Zheng, S. J. Zhang, and T. R. Shrout, *Appl. Phys. Lett.* **88**, 212908 (2006).

¹²R. Z. Zuo, J. Fu, and D. Y. Lv, *J. Am. Ceram. Soc.* **92**, 283 (2009).

¹³S. J. Zhang, R. Xia, T. R. Shrout, G. Z. Zang, and J. F. Wang, *J. Appl. Phys.* **100**, 104108 (2006).

¹⁴W. F. Liang, W. J. Wu, D. Q. Xiao, and J. G. Zhu, *J. Am. Ceram. Soc.* **94**, 4317 (2011).

¹⁵K. Wang, F. Z. Yao, W. Jo, D. Gobeljic, V. V. Shvartsman, D. C. Lupascu, J. F. Li, and J. Rödel, *Adv. Funct. Mater.* **23**, 4079 (2013).

¹⁶R. Zuo and J. Fu, *J. Am. Ceram. Soc.* **94**, 1467 (2011).

¹⁷J. Fu, R. Z. Zuo, S. C. Wu, J. Z. Jiang, L. Li, T. Y. Yang, X. H. Wang, and L. T. Li, *Appl. Phys. Lett.* **100**, 122902 (2012).

¹⁸Y. Saito, H. Takao, T. Tani, T. Nanoyama, K. Takatori, T. Homma, T. Nagaya, and M. Nakamura, *Nature (London)* **432**, 84 (2004).

¹⁹X. Wang, J. Wu, D. Xiao, J. Zhu, X. Cheng, T. Zheng, B. Zhang, X. Lou, and X. Wang, *J. Am. Chem. Soc.* **136**, 2905 (2014).

- ²⁰F. Z. Yao, Q. Yu, K. Wang, Q. Li, and J. F. Li, *RSC Adv.* **4**, 20062 (2014).
- ²¹E. K. Akdoğan, K. Kerman, M. Abazari, and A. Safari, *Appl. Phys. Lett.* **92**, 112908 (2008).
- ²²E. Hollenstein, D. Damjanovic, and N. Setter, *J. Eur. Ceram. Soc.* **27**, 4093 (2007).
- ²³S. J. Zhang, R. Xia, and T. R. Shrout, *Appl. Phys. Lett.* **91**, 132913 (2007).
- ²⁴T. A. Skidmore, T. P. Comyn, and S. J. Milne, *Appl. Phys. Lett.* **94**, 222902 (2009).
- ²⁵Y. Chang, S. Poterala, Z. Yang, and G. L. Messing, *J. Am. Ceram. Soc.* **94**, 2494 (2011).
- ²⁶J. Fu, R. Z. Zuo, and Z. K. Xu, *Appl. Phys. Lett.* **99**, 062901 (2011).
- ²⁷R. Z. Zuo, J. Fu, X. H. Wang, and L. T. Li, *J. Mater. Sci.: Mater. Electron.* **21**, 519 (2010).
- ²⁸H. Z. Guo, S. J. Zhang, S. P. Beckman, and X. L. Tan, *J. Appl. Phys.* **114**, 154102 (2013).
- ²⁹J. Yao, J. Li, D. Viehland, Y. Chang, and G. L. Messing, *Appl. Phys. Lett.* **100**, 132902 (2012).
- ³⁰D. Damjanovic, *J. Am. Ceram. Soc.* **88**, 2663 (2005).
- ³¹H. J. Trodahl, N. Klein, D. Damjanovic, N. Setter, B. Ludbrook, D. Rytz, and M. Kuball, *Appl. Phys. Lett.* **93**, 262901 (2008).
- ³²X. Ren, *Nat. Mater.* **3**, 91 (2004).
- ³³Z. Feng and X. Ren, *Phys. Rev. B* **77**, 134115 (2008).